Computational analysis of epilepsy-associated genetic mutations

Alberto De Marchi* and Ricardo Cervantes Casiano†

August 15, 2017

Abstract

In the central nervous system, the elementary processing unit are the neurons, they work together and are connected to each other in a very complicated pattern. In the brain, the most common disease is the epilepsy which is produced by abnormal electrical activity, and even a single gene mutation can cause the disease. Since neurons works together, we developed a network in such a way it compares the activity of control and mutated neurons working in a group. The basis of the neural network was the leaky integrate and fire model which describes the neuron by its membrane voltage potential; it uses the current threshold which is a fundamental ingredient for the modeling of the neuron. The measure of the network spikes was chosen to be the Fano factor. In our case, a higher Fano factor means higher the activity is in the network.

1 Introduction

Research in neuroscience over the last hundreds of years has accumulated an enormous amount of detailed knowledge about the structure and function of the brain. The most common neurological disease is epilepsy which is a collection of neurological disorders produced by abnormal electrical activity in the brain. As electrical activity is related to ion-channels (in particular the sodium channel) combined with the fact that single gene mutations can cause this disease, epilepsy associated mutations (GEFS+) are worth studying. In the brain, the elementary processing unit in the central nervous system are neurons, they work together and are connected to each other in a very complicated pattern. The structure of a neuron consists of the dendrites (play the role of input that collect signals from other neuron), the soma (central processing unit that performs important non-linear processing steps) and the axon (play the role of the output provided the total input exceed a threshold). The synapse is the junction between two neurons, and it is common to call the pre-synaptic cell to the neuron that sends the signal across the synapse. We call the post-synaptic cell to the neuron receiving the signal. It is worth mentioning that while the firing rate of a single neuron has the clearest signature that describes a process; evidence indicates that group of neurons working together might be an important component of the neural code. Here, we consider how gene mutations can affect a neural network.

*University of the German Federal Armed Forces; Munich, DE; alberto.demarchi@unibw.de

†University of Notre Dame; Notre Dame, USA.

2 Methods

In the following we denote with N the sodium channel averaged model proposed in Hay et al. (2011) with parameters adopted by Mäki-Marttunen et al. (2015), with wild-type (WT) the healthy SCN1A subunit of sodium channels and with H and G the subunit related to R859H and R865G mutations respectively (Volkers et al., 2011). Steady-state activation and inactivation curves of WT, H, G and N are shown in Fig. 1.

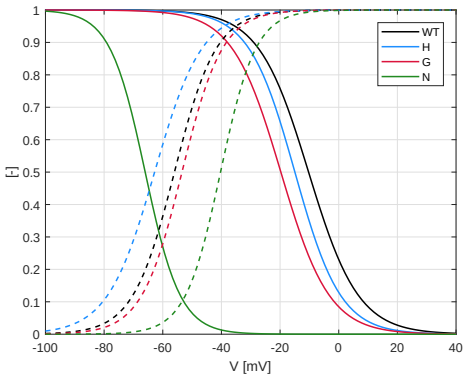

Figure 1: Steady-state activation and inactivation curves for N, WT, G and H; data from Volkers et al. (2011) and Mäki-Marttunen et al. (2015).

2.1 Model-to-model parameters fitting

In the work of Volkers et al. (2011), mathematical model with corresponding parameters are given to characterize the SCN1A sodium channel subunit. These parameters are available for WT, H and G.

An implementation of sodium channel based on the model proposed in Hay et al. (2011) and revisited in Mäki-Marttunen et al. (2015) is available for the `Neuron` simulator (Carnevale & Hines, 2006). Then, a set of parameters for this model has been found by fitting steady-state activation and inactivation curves and results from recovery after inactivation predicted by the two model. Least-squares fitting has been constrained to avoid unphysical results and carried out by using a genetic algorithm for global optimization. Results are shown in Fig. 2.

2.2 Current threshold matching

Averaged model is composed of N-type only, with maximum conductance $\overline{g}$, given in Mäki-Marttunen et al. (2015), while mixed model has both N and WT channels (N and H or G when mutated). We assume that in the mixed model conductances are respectively $\alpha\overline{g}$ and $\beta\overline{g}$, $0 < \alpha, \beta < 1$. Given a set of parameters $\mathcal{P}$ from previous fitting, it is possible using `Neuron` to estimate the *current threshold* I_{th}, i.e. the minimum current that makes the neuron to spike, for any tuple $(\mathcal{P}, \alpha, \beta)$. Here we are focusing on the current threshold because it is a fundamental parameter within the leaky-integrate-and-fire model of neuron behavior, adopted in the following part to build a neural network simulator. To carry out this and the following steps with the `Neuron` software, an interface with `MATLAB` has been created to easily set up and run simulations. For the current threshold estimation, the simulated time is 500 ms and the adopted protocol consists of a current injection of constant amplitude I in the time interval 100-350 ms. Neuron membrane potential is recorded and analyzed in `MATLAB`, identifying peaks with the built-in function `findpeaks`. A bisection search algorithm has been implemented to estimate the current threshold until a specified uncertainty.

The averaged model has threshold $I_{\text{th,N}} = I_{\text{th}}(\mathcal{P}, 1, 0)$ by definition (in fact for any $\mathcal{P}$). Then, selecting reasonable values of α, say $\alpha_k \in (0, 1)$, $k = 1, 2, \ldots$, we look for a corresponding sequence of values β_k such that

$$I^k_{\text{th,WT}} = I_{\text{th}}(\mathcal{P}_{\text{WT}}, \alpha_k, \beta_k) = I_{\text{th,N}} \tag{1}$$

for any $k \in \mathbb{N}$. Once the matching with the wild-type is done, we have the conductances of averaged channel and SCN1A subunit. These do not change if the mutations are present instead of the wild-type. Then, we can estimate the threshold of the variants, $X \in \{\text{H}, \text{G}\}$, for any $k \in \mathbb{N}$, namely

$$I^k_{\text{th},X} = I_{\text{th}}(\mathcal{P}_X, \alpha_k, \beta_k) \tag{2}$$

We expect to find $I^k_{\text{th},X} < I^k_{\text{th,WT}}$, $X \in \{\text{H}, \text{G}\}$ and for any $k \in \mathbb{N}$, because of the higher excitability of epileptic brains.

2.3 Relationship between applied current and firing rate

It is interesting to analyze the neuron dynamic response as a function of the stimulus. This is commonly evaluated by mean of the *f-I curve*, i.e. plotting the firing rate against the applied current. For the firing rate estimation, the simulated time in `Neuron` is 2000 ms and the adopted protocol consists of a current injection of constant amplitude I in the time interval 100-1850 ms. Peaks are identified in `MATLAB` from the recorded membrane potential. Then, the inter-spike time is adopted to estimate the spiking frequency. If only few spikes are fired, the estimation is quite uncertain and a longer simulation should be run. The resulting f-I curves are depicted in Fig. 3.

2.4 Leaky Integrate-And-Fire model

The leaky integrate and fire (LIAF) model consist of a linear differential equation that describe the evolution of the membrane potential and a threshold for spike firing. These spikes, so-called action potentials or pulses, have an amplitude of about 100 mV and typically a duration of 1-2 ms. This model is highly simplified and neglects many aspects of neuronal dynamics, such as long-lasting refractoriness or adaptation (it has one universal voltage threshold). However, the leaky integrate and fire model is surprisingly accurate when it comes to generating spikes. Thus, it can be used as a valid model of spike generation in neurons. The governing equation of neuron membrane potential V is

$$\tau \frac{\mathrm{d}V}{\mathrm{d}t} + V = E + RI \tag{3}$$

where τ and R respectively denote the time constant and resistance of neuron membrane, parameter E is the neuron resting potential and I is the current stimulating the neuron. Denoting t_{sp} the time at which the threshold potential is reached and a spike is fired, the reset dynamics within the LIAF model reads

$$\lim_{t \to t_{\text{sp}}^-} V(t) = V_{\text{th}} \tag{4}$$

$$\lim_{t \to t_{\text{sp}}^+} V(t) = V_{\text{reset}} < V_{\text{th}} \tag{5}$$

An absolute refractory period can be modelled by assuming that $V(t) = V_{\text{reset}}$ holds for any time instant $t \in (t_{\text{sp}},\ t_{\text{sp}} + T_{\text{refr}}]$, where T_{refr} is the refractory period duration.

Current I may consist of several contributions, e.g. synaptic current I_{syn}, applied current I_{stim} and non-specific background noise I_{b}. Focusing on a specific neuron in a network of n neurons, synaptic current I_{syn} depends on internal connections and is

modeled as a sum of post-synaptic currents from all of the other neurons in the network which have connections targeting the given neuron (Tsodyks et al., 2000), namely

$$I_{\text{syn}}(t) = \sum_{j=1}^{n} A_j y_j(t) \tag{6}$$

where A_j is a parameter describing the maximum strength of the connection with the j-th (pre-synaptic) neuron. The effective synaptic strength is determined by the state y, which is the fraction of synaptic resources in the active state. For each neuron, state y evolves according to the system of kinetic equations:

$$\frac{\mathrm{d}x}{\mathrm{d}t} = \frac{z}{\tau_{\text{rec}}} - ux\delta(t - t_{\text{sp}}) \tag{7}$$

$$\frac{\mathrm{d}y}{\mathrm{d}t} = -\frac{y}{\tau_{\text{I}}} + ux\delta(t - t_{\text{sp}}) \tag{8}$$

$$\frac{\mathrm{d}z}{\mathrm{d}t} = \frac{y}{\tau_{\text{I}}} - \frac{z}{\tau_{\text{rec}}} \tag{9}$$

where states x and z are the fractions of synaptic resources in the recovered and inactive states, respectively (Tsodyks et al., 2000). Parameter τ_{I} is the decay constant of PSCs and τ_{rec} is the recovery time from synaptic depression. Notice that $0 \leq x, y, z \leq 1$ and $\mathrm{d}x/\mathrm{d}t + \mathrm{d}y/\mathrm{d}t + \mathrm{d}z/\mathrm{d}t = 0$ at any time instant. Finally, state u describes the effective use of synaptic resources of the synapses. In facilitating synapses, it is increased with each pre-synaptic spike and returns to the baseline value with a time constant of τ_{facil}. The equation that characterize the evolution of u is

$$\frac{\mathrm{d}u}{\mathrm{d}t} = -\frac{u}{\tau_{\text{facil}}} + U(1-u)\delta(t - t_{\text{sp}}) \tag{10}$$

where the parameter U determines the increase in the value of u_i with each spike (Tsodyks et al., 2000).

In order to be used, parameters of the LIAF model, such as τ, R and V_{reset}, have to be estimated. To this end, we used the f-I curves obtained from `Neuron`. Because of its simplicity, within the LIAF model it is possible to derive analytically the f-I curve. For a constant applied current I, we can integrate (3) between two consecutive spikes. Taking into account the refractory period T_{refr} and denoting T the period between two consecutive spikes, the following condition is obtained

$$V_{\text{th}} = E + RI + [V_{\text{reset}} - E - RI]e^{-(T - T_{\text{refr}})/\tau} \tag{11}$$

Also constraints $V_{\text{th}} > E$, $V_{\text{th}} > V_{\text{reset}}$, $\tau > 0$ and $R > 0$ must hold. Notice that $V_{\text{th}} = E + RI_{\text{th}}$, by setting $\mathrm{d}V/\mathrm{d}t = 0$ at $V = V_{\text{th}}$. Introducing $\Delta = V_{\text{th}} - V_{\text{reset}}$ and rearranging (11), for $I > I_{\text{th}}$, the inter-spike interval T is given by

$$T = T_{\text{refr}} + \tau \ln\left(1 + \frac{\Delta}{R(I - I_{\text{th}})}\right) \tag{12}$$

and the firing rate is $f = T^{-1}$. Given previously estimated current threshold, it is possible to fit parameters τ, Δ and R of LIAF model to f-I curve obtained by using `Neuron`. Results of this fitting are shown in Fig. 4.

2.5 LIAF model and neural network

Let us consider a network of n neurons, connected with probability $p = 0.1$ (Tsodyks et al., 2000). Each neuron is described by its membrane potential and synaptic resources. Within this work, a simplified version of the model in Tsodyks et al. (2000) is adopted. Here we consider the i-th neuron to be uniquely characterized by V_i, x_i, y_i, z_i and u_i, whose dynamics are described by (3)–(10). Each neuron may have different parameters. Network topology and connections strength can be stored in an adjacency matrix $A \in \mathbb{R}^{n \times n}$. From (6), synaptic current to the i-th neuron is

$$I_{\text{syn},i}(t) = \sum_{j=1}^{n} A_{ij} y_j(t) \tag{13}$$

Entry A_{ij} of matrix A represents the connection strength from j-th to i-th neuron; its value is positive, A_{exc}, (negative, A_{inh}) if the j-th neuron is excitatory (inhibitory). The continuous-time membrane potential evolution of the i-th neuron is described by

$$\tau_i \frac{\mathrm{d}V_i}{\mathrm{d}t} + V_i = E_i + \epsilon_i + R_i\left(I_{\text{syn},i} + I_{\text{stim},i}\right) \tag{14}$$

where $\epsilon_i = RI_{\text{b},i} \sim \mathcal{N}(0, \sigma^2_{V,i})$ is a background time-varying voltage zero-mean i.i.d. Gaussian noise with $\sigma^2_{V,i}$ variance.

2.6 Network excitability and burstiness

Network activity a is computed as the relative number of neurons that fire an action potential during consecutive time bins of duration Δt (Tsodyks et al., 2000). Also, the Fano factor F is adopted as a measure of burstiness. It is defined as the ratio between variance σ^2 and mean value μ of a signal. In this work, we have considered the Fano factor of the network activity a, namely $F[a] = \sigma^2[a]/\mu[a]$.

Network activity and burstiness have been evaluated for a wide range of excitatory strength A_{exc} and background voltage noise standard deviation σ_V; inhibitory strength A_{inh} was assumed and set equal to zero (no inhibitory neurons), because former results are valid only for excitatory neurons. For any couple $(\sigma_V, A_{\text{exc}})$, values of a and $F[a]$ have been estimated based on n_{sims} simulations with randomly generated topologies and $\pm 1\%$ i.i.d. Gaussian noise on parameters.

3 Results

Parameters fitting between models is shown by comparing steady-state activation and inactivation curves and current of recovery after inactivation predicted by the two models with the corresponding parameters. In Fig. 2 the results are shown for a Monte Carlo simulation with noise on reference parameters, that were constrained to be between 80% and 120% the values of the averaged model in Mäki-Marttunen et al. (2015). Using `Neuron` with

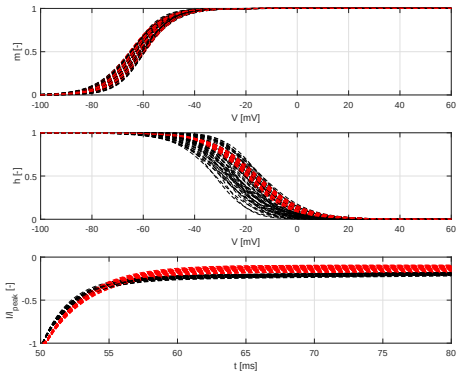

Figure 2: Monte Carlo analysis: fitting for WT, ±5% i.i.d. Gaussian noise.

the averaged model, we found the current threshold for N (0.328-0.329 nA) and matched the value of conductance to obtain the same current threshold for the mixed model with WT, obtaining e.g. $\beta = 8 \times 10^{-6}$ for $\alpha = 0.9$. In the following we will refer only to this couple of values. Using previous fitting results, the current threshold has been estimated for G and H, respectively 0.218-0.219 nA and 0.051-0.052 nA.

Now that the current thresholds have been obtained for WT and the variants, we can proceed to see how is the behavior of the dynamics. In Fig.3 the results shows that the current threshold for the G and H variant are both lower than the current threshold for the WT. In the case of the G variant, its curve overlap with the WT, so they are comparable in behavior. It is expected higher firing rate from the H and the G variant than the WT variant, making them more excitable. In Fig. 4 results shows how the LIAF model fit the values obtained using `Neuron` making it reasonable for utilization as descriptor of spikes times in a neuron. For the network simulator, we use $n = 100$ neurons and $n_{\text{sims}} = 40$ simulations. For the network activity it was adopted $\Delta t = T_{\text{refr}}$, where the refractory time was set $T_{\text{refr}} = 2$ ms. As a result, variants G and H show significant network activity at lower noise level than WT, Fig. 5 (not depicted for H). Furthermore, it can be seen from Fig. 6 that network burstiness, measured by the Fano factor F, behaves

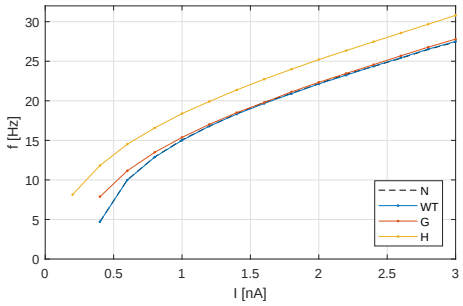

Figure 3: f-I curves of N, WT, G and H; for $\alpha = 0.9$ and $\beta = 8 \times 10^{-6}$.

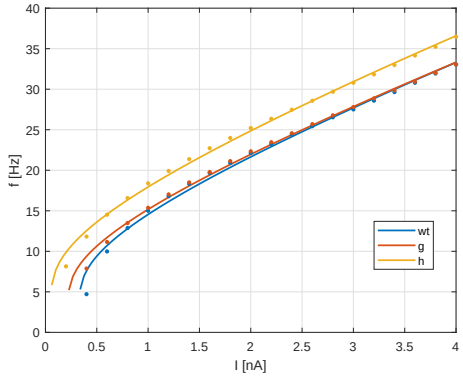

Figure 4: f-I curve fitting in frequency domain

qualitatively the same for WT, G and H, but moved to lower noise levels for the mutations.

4 Conclusions

At the neuron level, variants show lower current threshold for spiking and higher firing rate w.r.t. the wild-type. This means that both H and G are more excitable than WT ($I_{\text{th,WT}} \approx 0.328$ nA). In particular, H ($I_{\text{th,H}} \approx 0.051$ nA) is much more excitable than G ($I_{\text{th,G}} \approx 0.218$ nA). Also, at the network level, variants H and G are more susceptible, i.e. given A_{exc} they start spiking at a lower noise level. However, the behavior is qualitatively unchanged for a wide range of excitatory strength and background noise.

Future works may include the direct use in `Neuron` of model presented in Volkers et al. (2011) and inhibitory neurons should also be addressed and implemented. Within the neural network simulator, more sophisticated models accounting for adaptability and non-linear interactions could be analyzed and adopted. Moreover, a more robust measure of burstiness should be defined for a wider range of network activity.

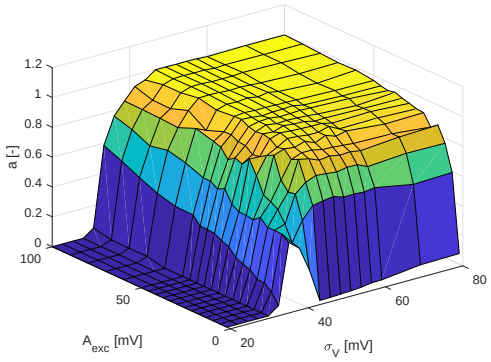

(a) WT

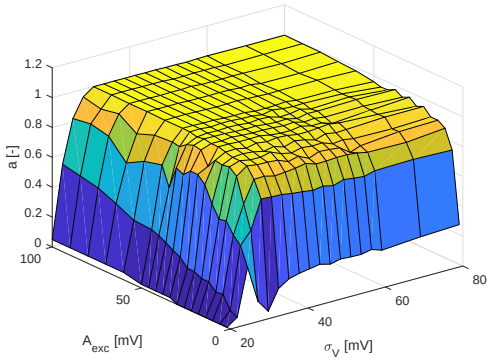

(b) G

Figure 5: Network activity a plotted against voltage noise standard deviation σ_V and excitatory strength A_{exc}, with $A_{\text{inh}} = 0$.

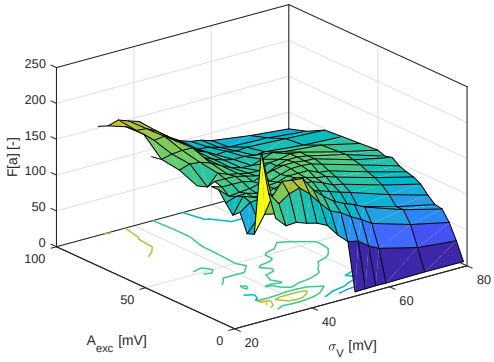

(a) WT

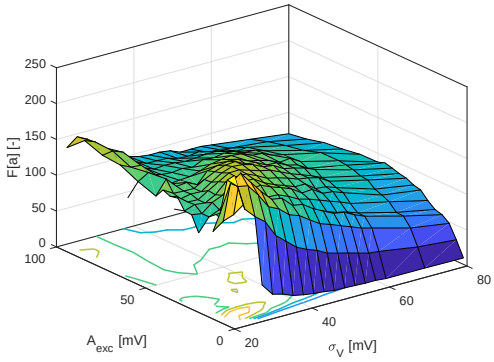

(b) G

Figure 6: Network burstiness: Fano factor $F[a]$ plotted against voltage noise standard deviation σ_V and excitatory strength A_{exc}, with $A_{\text{inh}} = 0$.

Acknowledgments

The authors are thankful to Tuomo Mäki-Marttunen for his guidance and supervision during the project work. Also, they would like to express special gratitude and appreciation to the University of Oslo, Simula Research Laboratory and the University of California, San Diego for giving them the opportunity to attend the 2017 Summer School in Computational Physiology.

References

Carnevale, N. T., & Hines, M. L. (2006). *The NEURON Book*. Cambridge, UK: Cambridge University Press.

Hay, E., Hill, S., Schürmann, F., Markram, H., & Segev, I. (2011). Models of neocortical layer 5b pyramidal cells capturing a wide range of dendritic and perisomatic active properties. *PLOS Computational Biology*, *7*(7), 1–18.

Mäki-Marttunen, T., Halnes, G., Devor, A., Witoelar, A., Bettella, F., Djurovic, S., Wang, Y., Einevoll, G. T., Andreassen, O. A., & Dale, A. M. (2015). Functional effects of schizophrenia-linked genetic variants on intrinsic single-neuron excitability: A modeling study. *ArXiv e-prints*.

Tsodyks, M., Uziel, A., & Markram, H. (2000). Synchrony generation in recurrent networks with frequency-dependent synapses. *Journal of Neuroscience*, *20*(RC50), 1–5.

Volkers, L., Kahlig, K. M., Verbeek, N. E., Das, J. H., van Kempen, M. J., Stroink, H., Augustijn, P., van Nieuwenhuizen, O., Lindhout, D., George Jr., A. L., Koeleman, B. P., & Rook, M. B. (2011). Na(v)1.1 dysfunction in genetic epilepsy with febrile seizures plus or dravet syndrome. *European Journal of Neuroscience*, *34*(8), 1268–1275.